Redistribution of reactive nitrogen in the Arctic lower stratosphere in the 1999/2000 winter

M. Koike, Y. Kondo, N. Takegawa, Franck Lefèvre, H. Ikeda, H. Irie, H. D. E. Hunton, A. A. Viggiano, T. M. Miller, J. O. Ballenthin, et al.

JOURNAL OF GEOPHYSICAL RESEARCH, VOL. 107, NO. D20, 8275, doi:10.1029/2001JD001089, 2002

Correction published 4 February 2003

Redistribution of reactive nitrogen in the Arctic lower stratosphere in the 1999/2000 winter

M. Koike,[1] Y. Kondo,[2] N. Takegawa,[2] F. Lefevre,[3] H. Ikeda,[2] H. Irie,[4] H. D. E. Hunton,[5] A. A. Viggiano,[5] T. M. Miller,[5] J. O. Ballenthin,[5] G. W. Sachse,[6] B. E. Anderson,[6] M. Avery,[6] and Y. Masui[1]

Received 10 July 2001; revised 27 November 2001; accepted 16 January 2002; published 14 September 2002.

[1] Total reactive nitrogen (NO_y) in the Arctic lower stratosphere was measured from the NASA DC-8 aircraft during the SAGE III Ozone Loss and Validation Experiment (SOLVE) in the winter of 1999/2000. NO_y-N_2O correlations obtained at altitudes of 10–12.5 km in December 1999 and January 2000 are comparable to the reported reference correlation established using the MkIV balloon measurements made during SOLVE prior to the onset of denitrification. Between late February and mid-March, NO_y values obtained from the DC-8 were systematically higher than those observed in December and January by up to 1 part per billion by volume, although a compact correlation between NO_y and N_2O was maintained. Greater increases in NO_y were generally observed in air masses with lower N_2O values. The daily minimum temperatures at 450–500 K potential temperature (~20–22 km) in the Arctic fell below the ice saturation temperature between late December and mid-January. Correspondingly, intense denitrification and nitrified air masses were observed from the ER-2 at 17–21 km and below 18 km, respectively, in January and March. The increases in NO_y observed from the DC-8 in late February/March indicate that influence from nitrification extended as low as 10–12.5 km over a wide area by that time. We show in this paper that the vertical structure of the temperature field during the winter was a critical factor in determining the vertical extent of the NO_y redistribution. Results from the Reactive Processes Ruling the Ozone Budget in the Stratosphere (REPROBUS) three-dimensional chemistry transport model, which reproduced the observed general features only when the NO_y redistribution process is included, are also presented. *INDEX TERMS:* 0340 Atmospheric Composition and Structure: Middle atmosphere—composition and chemistry; 0341 Atmospheric Composition and Structure: Middle atmosphere—constituent transport and chemistry (3334); 9315 Information Related to Geographic Region: Arctic region; *KEYWORDS:* reactive nitrogen, NO_y, Arctic, ozone, denitrification, nitrification

Citation: Koike, M., et al., Redistribution of reactive nitrogen in the Arctic lower stratosphere in the 1999/2000 winter, *J. Geophys. Res.*, *107*(D20), 8275, doi:10.1029/2001JD001089, 2002.

1. Introduction

[2] During the recent cold winters of the 1990s, such as 1994/1995, 1995/1996, and 1996/1997, significant ozone (O_3) loss was observed in the lower stratosphere in the Arctic. At temperatures below the nitric acid trihydrate (NAT) particle saturation point (T_{NAT}), liquid or solid particles (polar stratospheric clouds, PSCs) form and chlorine activation occurring on them results in subsequent catalytic photochemical O_3 destruction [*World Meteorological Organization* (*WMO*), 1999, and references therein]. Formation of PSC particles also causes nitric acid (HNO_3) uptake, leading to significant decreases in gas phase total reactive nitrogen (NO_y) concentrations [*Carslaw et al.*, 1994, 1997; *Drdla et al.*, 1994; *Tabazadeh et al.*, 1994; *Del Negro et al.*, 1997]. Denitrification, defined as the permanent removal of NO_y from an air mass by the sedimentation of PSCs, maintains high chlorine levels after temperatures warm to above the threshold temperature of PSC formation. Consequently, it delays deactivation of chlorine, extending ozone depletion through the late winter and into early spring [*Salawitch et al.*, 1993; *Rex et al.*, 1997; *Tabazadeh et al.*, 2000].

[3] Denitrification was observed in the Arctic stratosphere during the cold winters of 1989/1990 [*Fahey et al.*, 1990], 1994/1995 [*Sugita et al.*, 1998; *Waibel et al.*, 1999], 1995/

[1]Department of Earth and Planetary Science, Graduate School of Science, University of Tokyo, Japan.
[2]Research Center for Advanced Science and Technology, University of Tokyo, Japan.
[3]Service d'Aeronomie, Institut Pierre-Simon Laplace, Paris, France.
[4]National Institute for Environmental Studies, Tsukuba, Ibaraki, Japan.
[5]Air Force Research Laboratory/Space Vehicles Directorate, Hanscom Air Force Base, Massachusetts, USA.
[6]NASA Langley Research Center, Hampton, Virginia, USA.

0148-0227/02/2001JD001089

Table 1. Summary of SOLVE DC-8/ER-2 Deployments

Deployment	Start Date	End Date	Number of Flights
		DC-8	
December	30 Nov. 1999	16 Dec. 1999	8
January	14 Jan. 2000	29 Jan. 2000	7
March	27 Feb. 2000	15 March 2000	8
		ER-2	
January	14 Jan. 2000	3 Feb. 2000	7
March	26 Feb. 2000	16 March 2000	6

1996 [*Hintsa et al.*, 1998], and 1996/1997 [*Kondo et al.*, 2000; *Irie et al.*, 2001]. The degree of denitrification in the Arctic vortex is generally less intense and has greater interannual variability than that in the Antarctic vortex. When large PSC particles fall to lower altitudes and encounter higher temperatures, they evaporate or sublime, producing local increases in HNO_3 (nitrification). Nitrification has been observed in the Arctic lower stratosphere from aircraft [*Hübler et al.*, 1990; *Kawa et al.*, 1992; *Hintsa et al.*, 1998] and satellite [*Kondo et al.*, 2000; *Irie et al.*, 2001] instruments. Nitrification can result in an enhancement of NO_2 through the photolysis of the enhanced HNO_3 and therefore reduce the ozone loss rate at these altitudes. Consequently, measurements of nitrification provide not only additional evidence of redistribution of reactive nitrogen but also insight into the photochemistry at altitudes below the denitrified layer. Limited measurements of nitrification, however, have left significant uncertainties in the degree of nitrification, its horizontal extent, and its seasonal evolution.

[4] The Arctic stratospheric vortex during the 1999/2000 winter, studied by the SAGE III Ozone Loss and Validation Experiment (SOLVE)/Third European Stratospheric Experiment on Ozone (THESEO) 2000 campaign, was characterized by unusually low temperatures, especially in December and January [*Manney and Sabutis*, 2000]. Several measurements conducted during this campaign show that significant ozone loss occurred in the Arctic stratosphere [*Richard et al.*, 2001; *Salawitch et al.*, 2002; *Newman et al.*, 2002, and references therein]. By the end of March 2000, O_3 decreased by up to 2.5 parts per million by volume (ppmv), corresponding to 70% O_3 loss in the lower stratosphere [*Sinnhuber et al.*, 2000; *Santee et al.*, 2000]. The larger than normal loss of O_3 in March 2000 was likely due to widespread denitrification [*Gao et al.*, 2001; *Sinnhuber et al.*, 2000; *Santee et al.*, 2000]. In fact, severe denitrification was observed from the ER-2 at 16–21 km between late January and mid-March [*Popp et al.*, 2001]. An average removal of more than 60% was observed in air masses throughout the core of the Arctic vortex. The severity of denitrification was comparable to that inferred from previous measurements using the ER-2 in the Antarctic polar vortex in 1987. *Fahey et al.* [2001] observed large PSC particles (10–20 μm in diameter) containing nitric acid over a large altitude range (16–21 km) and horizontal extent from the end of January to the beginning of March. These large particles could fall 1.5 km/day and they are considered to be responsible for denitrification in the 1999/2000 Arctic winter.

[5] During the SOLVE campaign, a series of aircraft measurements in the lowermost part of the stratosphere at altitudes between 10–12.5 km (potential temperature of 300–360 K) were made using the NASA DC-8 aircraft from Kiruna, Sweden. Measurements were made during three phases from December 1999 to March 2000 (Table 1). Summaries of individual flights are given in the overview paper by *Newman et al.* [2002]. In situ measurement of NO_y was made along with various other species and physical parameters. In this paper, NO_y-N_2O correlations obtained in these three deployments are presented, and the causes of changes in the correlations are discussed.

2. Measurements and Chemical Transport Model

2.1. Measurements

[6] A schematic diagram of the DC-8 NO_y instrument used during SOLVE is shown in Figure 1. NO_y concentration was measured using an NO-O_3 chemiluminescence technique after NO_y compounds were catalytically converted into NO on the surface of a heated gold tube with the addition of CO. The NO_y instrument used for SOLVE was very similar to that used during NASA's Subsonic Assessment (SASS) Ozone and NO_x Experiment (SONEX) conducted in 1997 [*Koike et al.*, 2000; *Kondo et al.*, 1997]. The main difference was the mounting of the NO_y catalytic converter. During SOLVE, the NO_y converter unit was placed outside the aircraft cabin so that the length of the Teflon tube between the air sample inlet and the converter was minimized. The Teflon tube upstream of the converter was heated to 40°C. The inlet tube for air sampling faced rearward, discriminating against particles of diameters larger than about 1 μm. The conversion efficiency of NO_2 in ambient air was checked approximately every hour during each flight to achieve an efficiency of 99 ± 1%. The conversion efficiency of HNO_3 was checked in the laboratory before and after each deployment and values higher than 95% were found. The data were recorded every 1 s and 10-s averages were used in this study. The precision of the 10-s NO_y measurements at 10 km estimated from photon count fluctuations (1-σ) was 4 parts per trillion by volume (pptv) for an NO_y value of 1000 pptv. The absolute accuracy was estimated to be 10% for the given NO_y values.

[7] In addition to the gas phase NO_y measurement, measurement of NO_y with the forward facing inlet was simultaneously made using an independent gold tube converter (Figure 1). With this configuration, HNO_3-containing particles were detected in addition to gas phase NO_y and this measurement is denoted as the total NO_y measurement. Except for the very limited cases in which PSC particles existed, NO_y and total NO_y measurements agreed to within the combined uncertainties throughout the three deployments. This good agreement between the two NO_y measurements ensure the overall performance of the NO_y measurements during the SOLVE experiment.

[8] Intercomparisons between the DC-8 and ER-2 aircraft measurements were made on 23 January 2000 during the SOLVE campaign. The two aircraft flew very close-track at an altitude of 11.3 km in the upper troposphere for about 25 min. The results of the intercomparison for 10-s NO_y data are shown in Figure 2. The time axis of the ER-2 data was adjusted so that data obtained at the same locations are

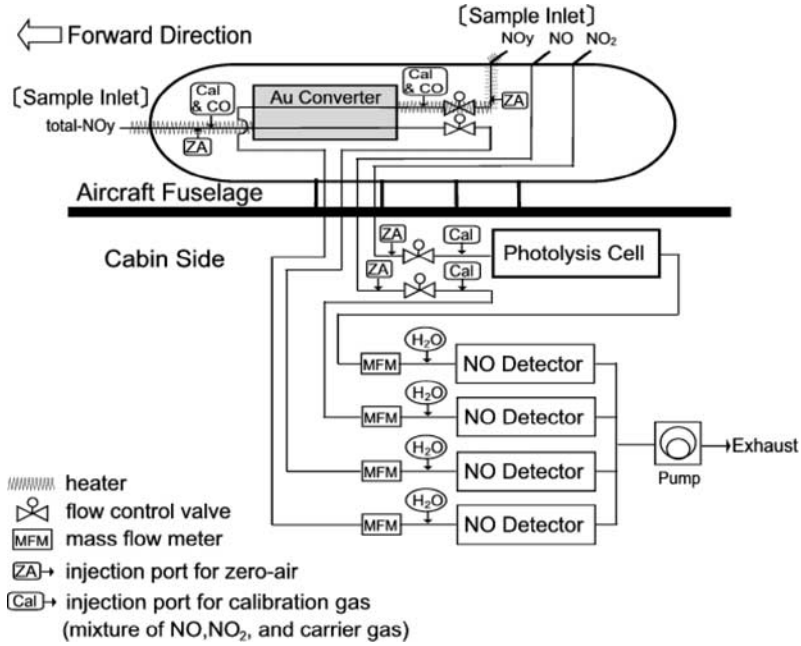

Figure 1. Schematic diagram of the instrument used to measure NO, NO_2, NO_y, and total NO_y (gas phase and aerosols) on board the DC-8 aircraft during SOLVE. The sample flow rate was controlled using a flow control valve and mass flow meter. A mixture of NO and N_2 gases (calibration gas) was injected with a carrier gas into the sample flow (denoted as "Cal" in the diagram) to calibrate the sensitivity and conversion efficiency during the calibration mode. During the other modes, calibration gas was continuously vented through the exhaust tubing. Zero air was also occasionally injected into the sample flow (denoted as "ZA" in the diagram).

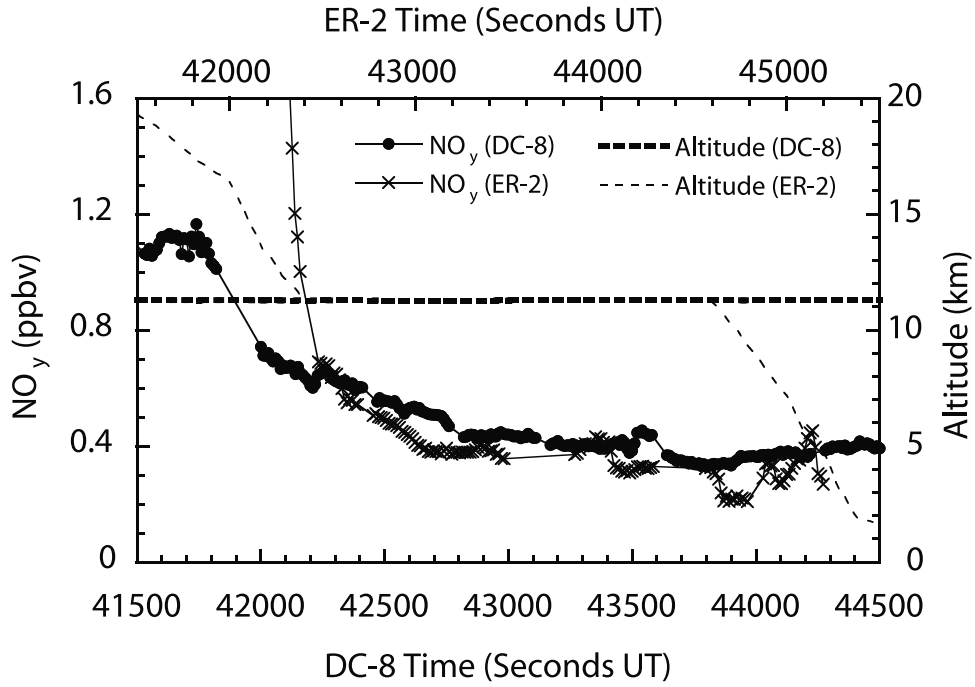

Figure 2. Intercomparison data from the ER-2 and DC-8 NO_y measurements obtained on 23 January 2000 at an altitude of 11.3 km (upper troposphere). Ten-second averages are shown. The time axis of the ER-2 data was adjusted so that data obtained at the same locations are overlaid. An averaged horizontal distance between the two measurements was 4.7 ± 2.1 km after this adjustment. The two measurements agreed to within 35 ± 42 pptv or 8.7 ± 9.8% (DC-8 measurements were higher).

overlaid. The average horizontal distance between the two measurements was 4.7 ± 2.1 km after this adjustment. As seen in this figure, the agreement between the two aircraft measurements was very good. On average, they agreed to within 35 ± 42 pptv or 8.7 ± 9.8% (the DC-8 measurements were higher), which was within the combined uncertainties of the two measurements.

[9] In this paper, N_2O data simultaneously obtained on board the DC-8 aircraft using a tunable diode laser absorption technique [*Vay et al.*, 1998] were used. Data were recorded at 1 Hz with a precision (1-σ) of 0.1% and an absolute accuracy better than 1% (2-σ). The O_3 measurements were made using a chemiluminescence technique with a precision (1-Hz measurement) of 2% or 1 parts per billion by volume (ppbv), whichever is larger, and an absolute accuracy of 2 ppbv. Data from the ER-2 aircraft measurements of NO_y [*Fahey et al.*, 1989] and N_2O are also used. Because three independent N_2O measurements were made on board the ER-2 aircraft, we used a combined N_2O data set (unified N_2O data) [*Hurst et al.*, 2002]. Typical agreement ranged from 3.6 to 7.3 pptv (1.8 to 3.7%) for the different instrument pairs, while the unified N_2O data agreed with whole air sample measurements within 2.9 ppbv (1.5%).

2.2. Chemistry Transport Model

[10] We used in our analysis the REPROBUS three-dimensional (3-D) Chemical Transport Model (CTM), which computes the time evolution of 55 stratospheric species [*Lefevre et al.*, 1994, 1998]. The chemistry package includes a comprehensive treatment of gas-phase chemistry (147 reactions and photolysis rates from JPL [*DeMore et al.*, 1997; *Sander et al.*, 2000]), as well as heterogeneous reactions taking place at the surface of liquid [*Carslaw et al.*, 1995] and solid PSCs. The model was initialized on October 15, 1999. The wind and temperature fields used to drive the transport of chemical species and to compute the chemical reaction rates were prescribed every six hours by the European Centre for Medium-Range Weather Forecasts (ECMWF) analysis. In the configuration used in our study, REPROBUS extends over 42 vertical levels from the ground up to 0.1 hPa (about 65 km altitude), with a horizontal resolution of 2° × 2° and a chemical time step of 15 min.

[11] The process leading to denitrification is also included in the REPROBUS model. When the temperature drops below T_{NAT} and a supersaturation ratio of 10 is achieved, NAT particles are allowed to form on a limited number of condensation nuclei (5×10^{-3} particles cm^{-3}), and they coexist with supercooled ternary solution (STS) droplets in much larger concentrations. This highly selective nucleation process leads to large NAT particles with a maximum diameter of about 10 μm, resulting in denitrification. Various sensitivity tests were performed to evaluate the impact of the assumed NAT number density, and the results will be presented in section 4.3. Note that because of the assumption of a supersaturation ratio of 10, NAT particle are allowed to form only when temperatures drop below T_{NAT} by 3 K at 50 hPa, which is about 192 K. This temperature is the edge of the "nucleation window" of 191 ± 1 K at 50 hPa, where production rates of nitric acid dihydrate (NAD) and NAT particles through the homogeneous freezing process are largest [*Tabazadeh et al.*, 2001]. When these large NAT particles fall to lower altitudes and encounter temperatures higher than T_{NAT}, they evaporate or sublime, causing nitrification.

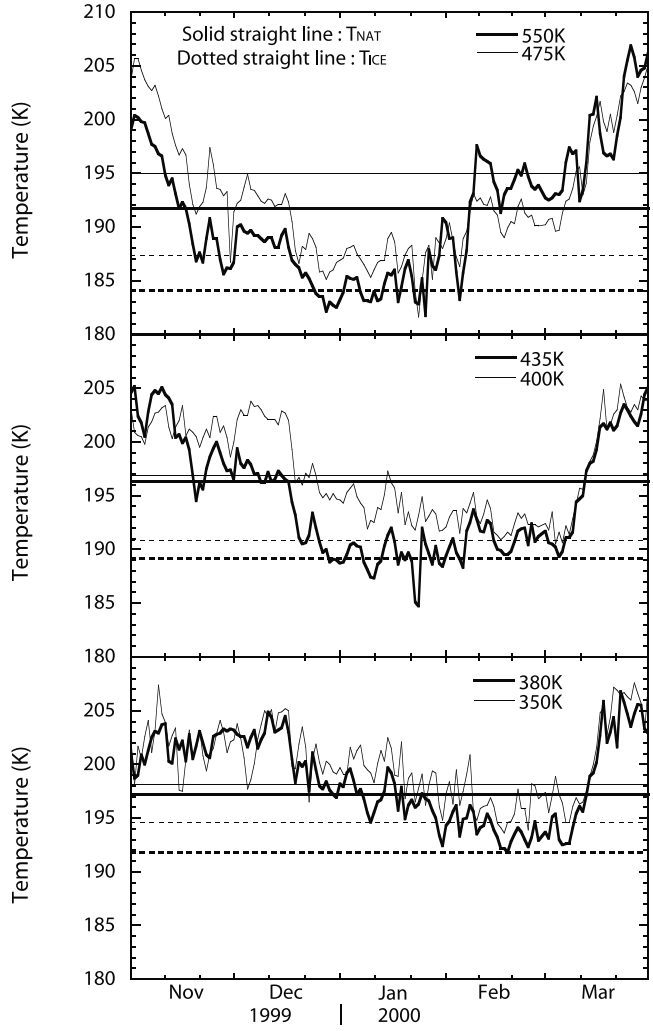

Figure 3. Minimum temperatures in the Northern Hemisphere (north of 45°N) at various potential temperature surfaces derived using ECMWF data. The threshold temperatures for the formation of nitric acid trihydrate (NAT) particles (T_{NAT}) and ice particles (T_{ICE}) are also shown.

3. Meteorological Conditions

[12] The 1999/2000 Arctic stratospheric vortex was characterized by unusually low temperatures, especially in December and January [*Manney and Sabutis*, 2000]. Figure 3 shows the minimum temperatures north of 45°N at various potential temperature levels from the ECMWF analyses. The threshold temperatures for the formation of NAT particles, T_{NAT}, and ice particles, T_{ICE}, are also shown in this figure. These values were calculated using the formula derived by *Hanson and Mauersberger* [1988] and *Marti and Mauersberger* [1993] and assuming the HNO_3 and H_2O mixing ratios used by *Irie et al.* [2001]. Figures 4a and 4b show the development of areas with temperatures below T_{ICE}

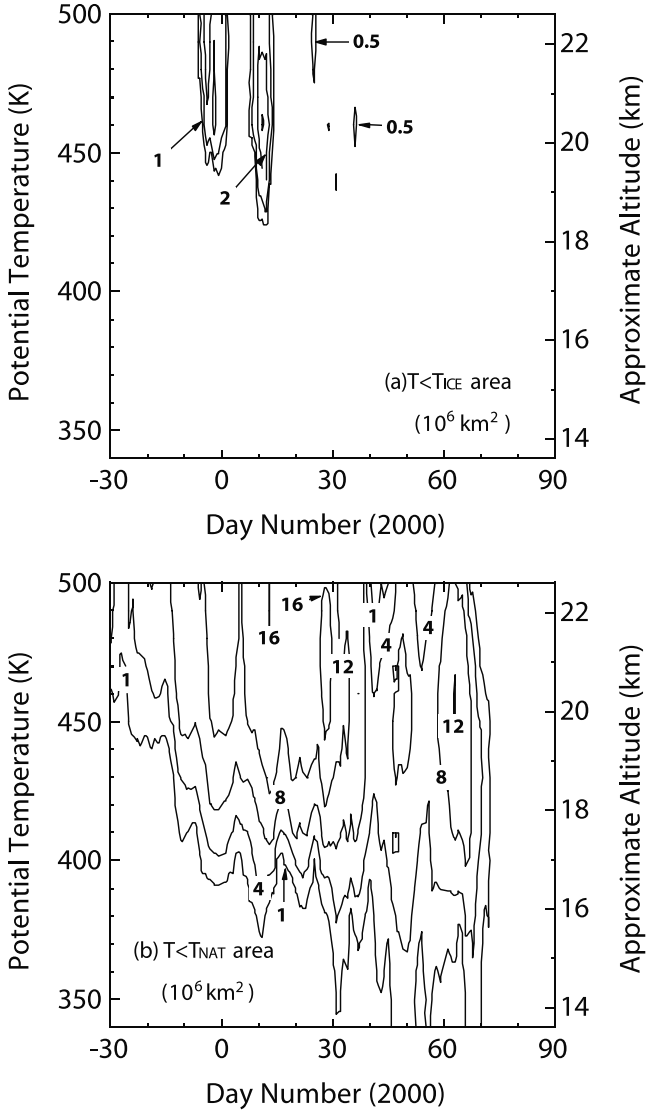

Figure 4. Development of areas with temperatures (a) below T_{ICE} and (b) below T_{NAT}.

and T_{NAT}, respectively. At 475 K (~21 km), where the ER-2 measurements were intensively made, the minimum temperature fell below T_{NAT} from the end of November to the beginning of March and below T_{ICE} at the end of December and the beginning of January. Between 450 and 500 K, the area where temperatures were below T_{NAT} covered close to half of the total Arctic vortex area of about 19×10^6 km^2 through January. At 350 K (~13.5 km), which is slightly higher than the altitude where the DC-8 measurements were intensively made, the minimum temperature fell well below T_{NAT} from the beginning of February to the beginning of March. At this altitude, areas in which temperatures occasionally fell below T_{NAT} in February correspond to 5% of the total vortex area. The time when the lowest temperatures appeared was generally observed later at lower altitudes.

[13] Corresponding to these low temperatures in entire Arctic stratosphere, extensive PSCs were observed over the course of the SOLVE campaign [*Newman et al.*, 2002, and reference therein]. These results suggest that large-scale low-temperature features were generally responsible for PSC formation during the 1999/2000 Arctic winter.

4. Results and Discussion

4.1. N_2O-NO_y Correlation Observed from DC-8

[14] Scatterplots between NO_y and N_2O obtained from DC-8 measurements during the December, January, and March deployments are shown in Figure 5. Median values

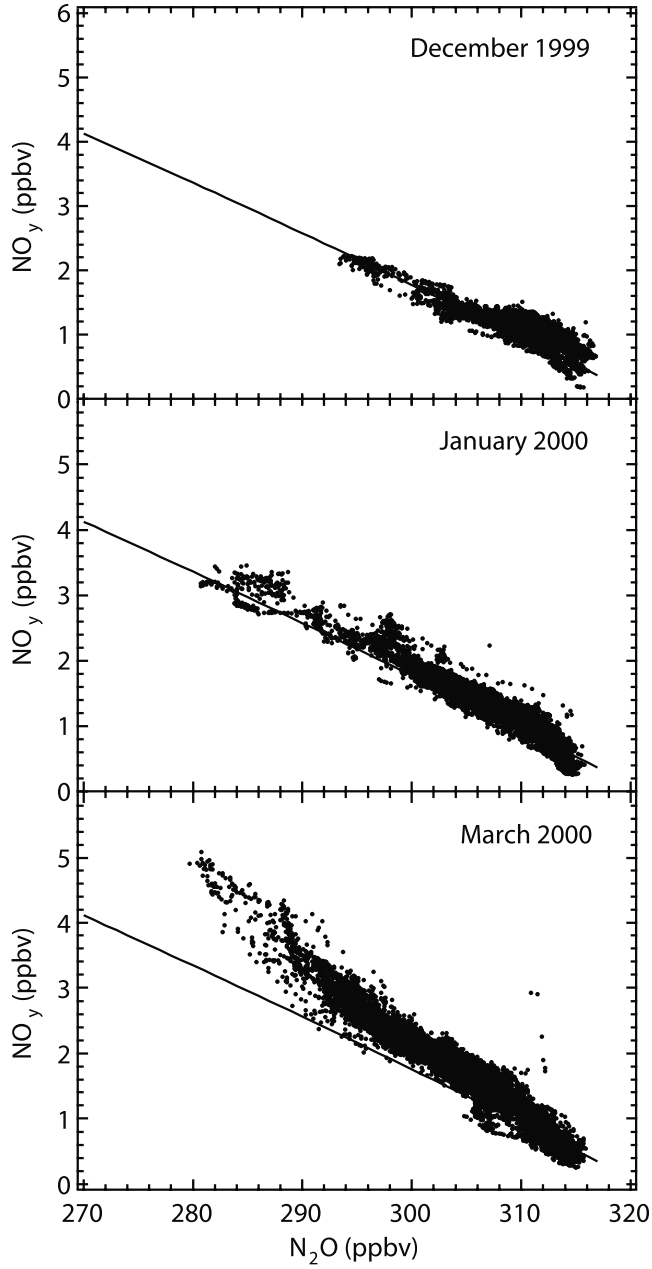

Figure 5. Scatterplots between NO_y and N_2O derived from the DC-8 measurements. Solid lines are the reference relationship obtained from the MkIV measurements (prior to the onset of denitrification), which is in good agreement with the ER-2 extravortex measurements (the relationship referred to as the SOLVE MkIV/ER-2 relationship in section 4.1, which is expressed by equation (1)).

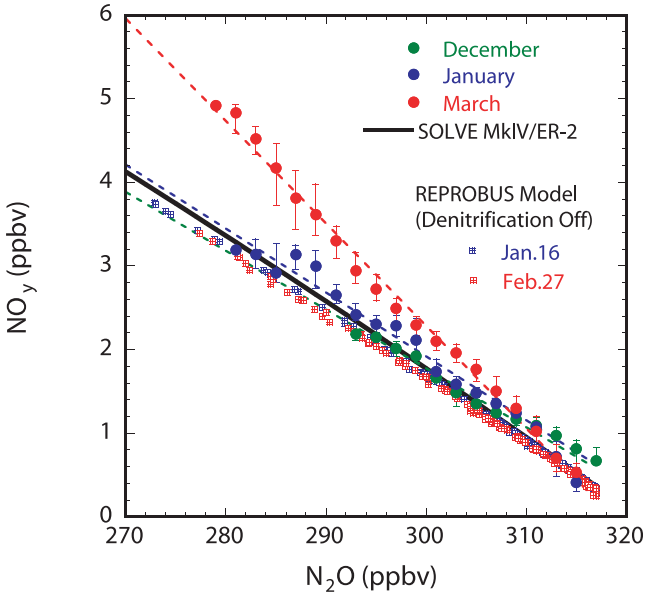

Figure 6. Median values of NO_y for various N_2O ranges obtained from the DC-8 measurements. The vertical bars are the 67% ranges of the NO_y values. In this plot, CTM-calculated NO_y and N_2O values along the DC-8 flight track are also shown for the 16 January (January deployment) and 27 February (March deployment) cases. In these model calculations, the process leading to denitrification was disabled (denitrification OFF) so that effects other than the NO_y redistribution process are seen.

of NO_y in each N_2O range are shown in Figure 6, and a linear regression line calculated for these median values is given in Table 2. In these figures, data obtained in stratospheric air masses (O_3 > 100 ppbv) sampled north of 50°N and above 5 km were used. *Popp et al.* [2001] established a reference N_2O-NO_y relationship for the 1999/2000 Arctic vortex using remote measurements obtained by the MkIV balloon-borne interferometer on December 3, 1999, prior to the onset of denitrification:

$$[NO_y^*] = 17.3 - (0.0222 \times [N_2O]) - (9.85 \times 10^{-5}) \times [N_2O]^2, \quad (1)$$

where both $[NO_y^*]$ and $[N_2O]$ are expressed in ppbv. The reference relationship was derived using data with N_2O values between 33 and 321 ppbv. The NO_y values measured from the ER-2 aircraft agreed well with the NO_y* values in air masses that had not been perturbed by denitrification or nitrification processes, and we will therefore refer to the above equation as the MkIV/ER-2 reference relationship. This reference relationship is shown in Figures 5 and 6. M. Loewenstein et al. (An NO_y* algorithm for Arctic winter 2000, submitted to *Journal of Geophysical Research*, 2001) also established a reference N_2O-NO_y relationship for the 1999/2000 Arctic winter for the entire N_2O range. Their NO_y* values for the N_2O = 60–320 ppbv range were quite similar to those derived using the equation (1).

[15] During the SOLVE campaign, the N_2O mixing ratios measured from the DC-8 ranged between 280 and 320 ppbv. The N_2O–NO_y relationship in December was in good agreement with the MkIV/ER-2 reference relationship. In January, although NO_y values increased slightly in air masses with N_2O mixing ratios of 290–300 ppbv, they were still in good agreement with the MkIV/ER-2 reference values. In contrast, NO_y values obtained in late February/March (March deployment) were systematically higher than those in December and January. The increase in NO_y values ($\Delta NO_y = NO_y - NO_y$*) was especially evident in air masses with N_2O values of 280–290 ppbv (altitudes of 11.0–12.5 km and potential temperatures of 340–350 K), where ΔNO_y values were 0.5 to 1 ppbv. These air masses were sampled during the five flights made from 27 February to 15 March. It should be noted that the linear correlation between NO_y and N_2O is quite compact in late February/March, as confirmed by small standard deviations in NO_y values (Figures 5 and 6). This indicates that air masses sampled in late February/March were generally well mixed with surrounding air masses.

[16] The highest values of NO_y and ΔNO_y, up to 5 and 1 ppbv, respectively, were observed on 27 February during the transit flight from the west coast of United States to Kiruna, Sweden. The locations in which these high NO_y values were observed are shown in Figure 7 with the Ertel's potential vorticity (EPV) field at the 217-hPa surface. As seen in this figure, these high-NO_y air masses were sampled in the regions where EPV values were relatively high on that pressure altitude.

[17] Possible causes that could alter the N_2O-NO_y correlation are now examined. In Figure 6, a scatterplot between the REPROBUS model-calculated NO_y and N_2O is shown for the 16 January and 27 February cases. In these calcu-

Table 2. Relationships Among N_2O, NO_y, and O_3[a]

	Deployment	Relationship	Uncertainty in the Slope (1-σ)	Uncertainty in the Intercept (1-σ)	r^2
NO_y-N_2O	Dec. 1999	$[NO_y(\text{pptv})] = -70.29\ ([N_2O(\text{ppbv})] - 316.6) + 609$	±4.27	±62	0.97
	Jan. 2000	$[NO_y(\text{pptv})] = -76.35\ ([N_2O(\text{ppbv})] - 316.6) + 653$	±3.47	±78	0.97
	March 2000	$[NO_y(\text{pptv})] = -122.47\ ([N_2O(\text{ppbv})] - 316.6) + 249$	±3.51	±79	0.99
O_3-N_2O	Dec. 1999	$[O_3(\text{ppbv})] = -24.42\ ([N_2O(\text{ppbv})] - 316.6) + 120$	±0.26	±4	1.00
	Jan. 2000	$[O_3(\text{ppbv})] = -23.13\ ([N_2O(\text{ppbv})] - 316.6) + 99$	±0.22	±5	1.00
	March 2000	$[O_3(\text{ppbv})] = -20.63\ ([N_2O(\text{ppbv})] - 316.6) + 126$	±0.27	±6	1.00
NO_y-O_3	Dec. 1999	$[NO_y(\text{pptv})] = -2.603\ ([O_3(\text{ppbv})] - 100) + 655$	±0.128	±41	0.98
	Jan. 2000	$[NO_y(\text{pptv})] = -3.558\ ([O_3(\text{ppbv})] - 100) + 536$	±0.108	±51	0.99
	March 2000	$[NO_y(\text{pptv})] = -5.534\ ([O_3(\text{ppbv})] - 100) + 288$	±0.193	±85	0.98

[a] These linear regression lines were calculated for median values, shown in Figures 6 and 8 for the case of the NO_y-N_2O and O_3-N_2O relationships. In the same way, the relationship between NO_y and O_3 was calculated for median values of NO_y for various O_3 ranges (50 ppbv intervals). When the regression lines were calculated, the value of 100 or 316.6 in the expression was kept fixed. The O_3 mixing ratio of 100 ppbv was chosen as a typical value at the tropopause. The N_2O mixing ratio of 316.6 ppbv is an average value in the troposphere during SOLVE.

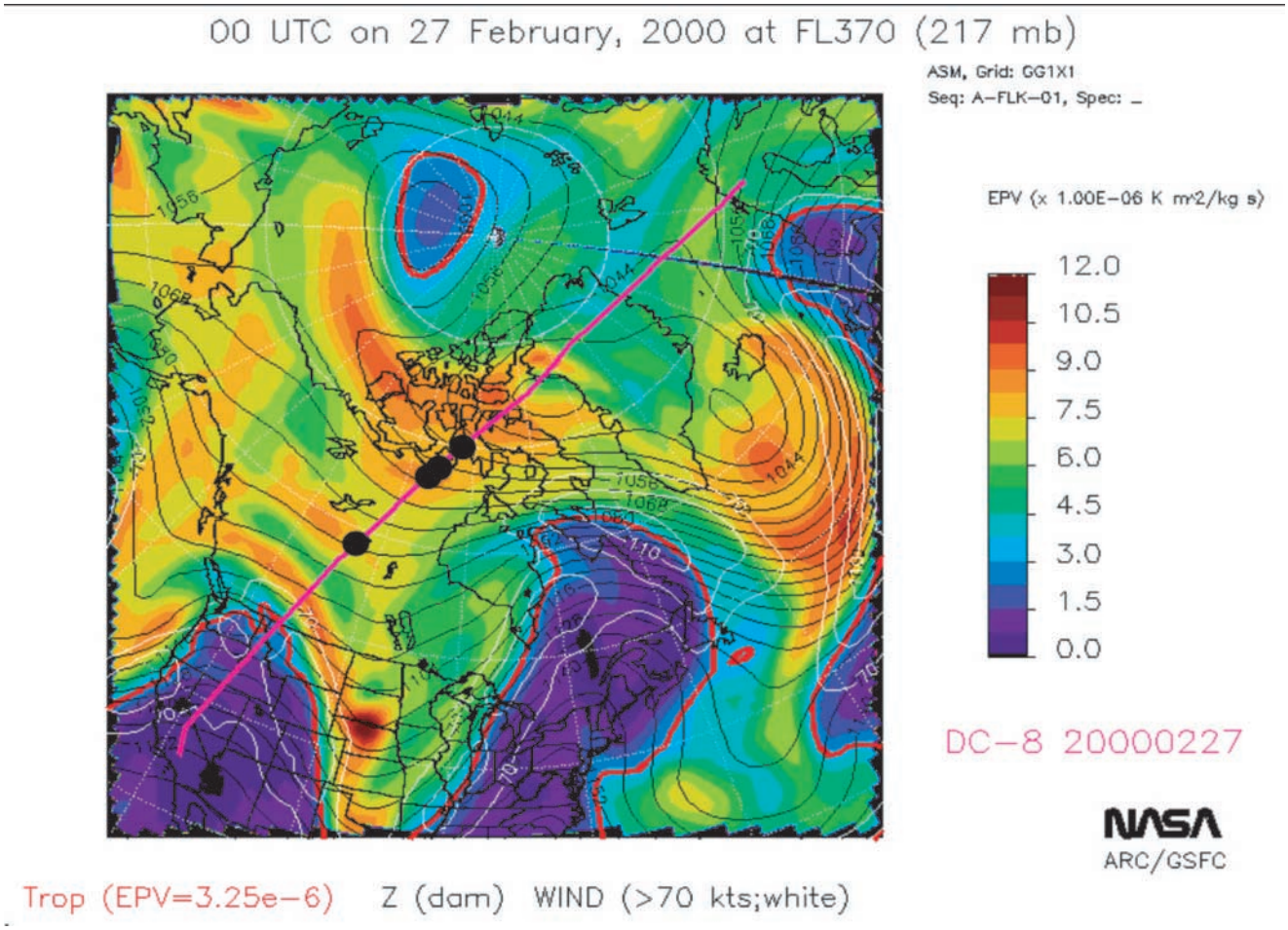

Figure 7. Flight track of the DC-8 on 27 February 2000 (purple line) overlaid on the GEOS-3 meteorological analysis at 217 hPa, prepared for the SOLVE mission by the Data Assimilation Office (DAO) at NASA Goddard Space Flight Center. Locations where NO_y values higher than 4 ppbv were observed are denoted with closed black circles. Analysis fields depicted here are Ertel's potential vorticity (EPV) in PV units (10^{-6} K m^2 kg^{-1} s^{-1}), geopotential height (black contours, intervals of 4 decameters or 40 m) and wind speed (white contours, intervals 20 knots, or $\sim$10 m s^{-1}.) Red lines indicate the intersection of the tropopause surface (here defined by EPV = 3.25 PV units) with the 217-hPa surface.

lations, the process leading to denitrification was disabled (model denitrification OFF), and model values along the DC-8 flight track were extracted. These two days were selected because 16 January (January deployment) was the day on which air masses with N_2O = 280–290 ppbv were observed with no increase in NO_y from the DC-8, while 27 February (March deployment) was the day on which air masses in the same N_2O range were observed with a clear increase in NO_y ($\sim$1 ppbv). The model-calculated NO_y-N_2O relationships are quite similar between the January and March cases. This result indicates that a seasonal change in the transport processes is not responsible for the observed change in the NO_y-N_2O relationship. The earlier ER-2 measurements also show that the NO_y-N_2O correlation at northern midlatitudes over the wider N_2O range (N_2O = 170–300 ppbv) changed little with season when intensive denitrification did not take place [*Keim et al.*, 1997].

[18] In Figure 8, median values of O_3 are shown versus N_2O using DC-8 data. A linear regression line calculated for these median values is given in Table 2. As seen in this figure and table, the relationship changed little between December and March and did not show any corresponding increase in O_3 in March as seen in the NO_y-N_2O relationship. This result further confirms that there was no change in the meridional transport, which can alter the NO_y-N_2O or O_3-N_2O relationship, in the DC-8 sampling area during the SOLVE campaign. Slight decreases in O_3 amount from December to March could be due to photochemical O_3 loss. In fact, the decrease of 63 ppbv (7.1%) in air masses with N_2O = 280 ppbv between the January and March deployments (44 days apart) is generally consistent with the photochemical O_3 loss of about 80 ppbv (9%) within the same period calculated using the REPROBUS model for N_2O = 280 ppbv air masses. An O_3 reduction of 60–130 ppbv (9–16%) was also observed during the AASE 2 experiment from the DC-8 between January and March 1992 in air masses with N_2O = 270–290 ppbv (at altitudes around 11.5 km) when the N_2O-O_3 correlation was used in the estimation [*Collins et al.*, 1993]. In addition to the N_2O-O_3 and NO_y-N_2O relationships, a relationship between NO_y and O_3 observed during SOLVE is given in Table 2 for reference.

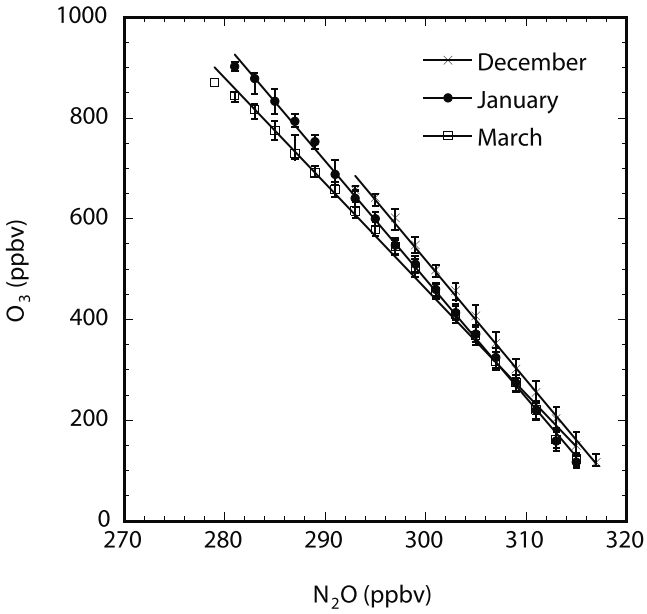

Figure 8. Relationship between O_3 and N_2O derived from the DC-8 measurements. Median values of O_3 for various N_2O ranges are shown. The vertical bars are the 67% ranges of the O_3 values.

[19] There are other possible causes that could alter the NO_y-N_2O correlation. First, it is very unlikely that the observed increase in NO_y in March was due to errors in the observations. The absolute values of the NO_y measurements were well calibrated with a NO standard gas, and no systematic change in the sensitivity was found throughout the three deployments. The conversion efficiency of HNO_3 was higher than 95% and, in fact, NO_y measurements agreed with independent measurements of total NO_y within the combined uncertainties, as described in section 2.1. Furthermore, the changes in sensitivity and HNO_3 conversion efficiencies cannot explain the observed N_2O dependence in the ΔNO_y values. Second, recent mixing of tropospheric air into the lower stratosphere cannot explain the observed increase in NO_y, because the NO_y values in the troposphere were mostly below 1 ppbv. Third, aircraft emissions can increase the NO_y level in the lower stratosphere; however, its contribution was estimated to be only 0.1–0.2 ppbv, even near the North Atlantic flight corridor [*Koike et al.*, 2000]. It was also suggested that their impact was largest near the tropopause region (O_3 = 75–125 ppbv), and it was generally smaller deeper inside the stratosphere. Therefore the increase in NO_y observed in late February/March was quite likely due to the vertical redistribution of NO_y in the Arctic vortex caused by the gravitational sedimentation of PSC particles. As seen in Figures 5 and 6, the NO_y value increased by changing the dNO_y/dN_2O gradient rather than by a constant offset. The N_2O dependence of the NO_y increase was reasonable, because air masses with lower N_2O values were expected to be affected more strongly by higher altitude air masses where nitrification was more intense. In the following sections (sections 4.2 and 4.3), redistribution of NO_y observed from the ER-2 and results from the 3-D REPROBUS model calculations are presented to confirm our interpretation.

4.2. N_2O-NO_y Correlation Observed from ER-2

[20] In Figure 9a, a scatterplot between N_2O and NO_y measured from the ER-2 aircraft is shown. For this plot, we used only data obtained at temperatures higher than T_{NAT}, to

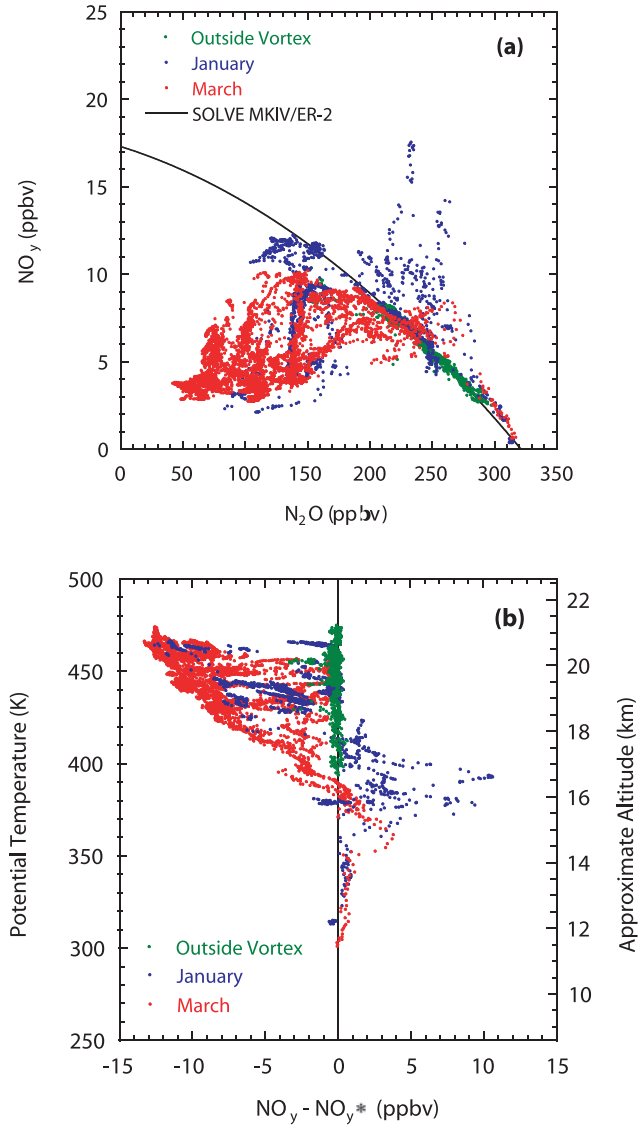

Figure 9. (a) Scatterplot between NO_y and N_2O derived from ER-2 measurements. (b) Vertical profile of redistributed NO_y ($\Delta NO_y = NO_y - NO_y^*$) derived from ER-2 measurements. For these plots, only data obtained at temperatures higher than T_{NAT} were used. Blue and red circles represent data obtained in the January and March deployments, respectively. For measurements made at altitudes higher than 15 km, extravortex data (those obtained outside the outer edge of the Arctic vortex) are shown using green circles, irrespective of the month when the measurements were made. The approximate altitude for inside-vortex measurements is shown on the right-hand side of the figure. Note that these two plots are nearly identical to those shown by *Popp et al.* [2001].

exclude measurements made when NO_y-containing PSC particles were present in the sampled air mass. For the T_{NAT} calculation, observed values of NO_y and H_2O were used, and all of NO_y was assumed to be HNO_3. In this figure, data obtained in the January and March deployments are shown using different colors (blue and red). For measurements made at altitudes higher than 15 km, data obtained outside the outer edge of the Arctic vortex, as determined using the definition of *Nash et al.* [1996], are shown using another color (green). These extra-vortex data agreed well with the MkIV/ER-2 reference relationship. Severe denitrification was observed between late January and mid-March 2000 at altitudes of 17–21 km and for N_2O mixing ratios between 40 and 170 ppbv, as reported by *Popp et al.* [2001]. They also reported that an average removal of NO_y of more than 60% was observed in air masses throughout the core of the Arctic vortex. Corresponding to the denitrification, nitrification was observed from the ER-2 both in January and March (Figure 9a). Increases in NO_y were as high as 10 ppbv in January.

[21] In Figure 9b, the vertical profile of redistributed NO_y ($\Delta NO_y = NO_y - NO_y^*$) derived from ER-2 measurements using the MkIV/ER-2 reference relationship (equation (1) given above) is shown using the same data set used for Figure 9a. As seen in this figure, denitrification was observed between 16 and 21 km, and maximum value of the NO_y removal in each altitude increased with altitude partly because the amount of available NO_y increased with altitude [*Popp et al.*, 2001]. The colder temperatures at higher altitudes (Figures 3 and 4) were also favorable for the efficient removal of NO_y. The vertical profile of maximum removal value shifted downward by 0.5–1 km from January to March between 18 and 21 km, although the number of measurements in January was small. This vertical shift was partly due to diabatic descent of air inside the Arctic vortex. In fact, vertical profiles of N_2O obtained from the ER-2 measurements shifted downward by 0.5–1 km (10–20 K potential temperature) from January to March at altitudes above 14 km, with higher descent rates at higher altitudes (not shown). This descent rate was generally consistent with the estimates from a more comprehensive study for the 1999/2000 Arctic winter [*Greenblatt et al.*, 2002], earlier measurements [*Schoeberl et al.*, 1992; *Abrams et al.*, 1996], and model calculations [*Rosenfield et al.*, 1994]. In addition to the descent of air masses, further denitrification, which occurred at lower altitudes in February, could also cause negative ΔNO_y values at 380–400 K. As seen in Figures 3 and 4, the minimum temperatures at 380–400 K (~15.5–17 km) were lower in February than in January and were close to T_{ICE} until the beginning of March. In fact, large HNO_3-containing PSC particles, which contributed significantly to denitrification, were detected until 7 March [*Fahey et al.*, 2001].

[22] Air masses with positive ΔNO_y values due to nitrification were occasionally observed from the ER-2. The number of measurements below 16 km was quite small because they were made only during ascent and descent from the Kiruna airport, and therefore the location of air mass sampling was also limited to the region over northern Scandinavia. Within this limited data set, nitrification was clearly seen at 15–18 km and 14–16.5 km in January and March, respectively. Increases in NO_y of 0.5–1 ppbv were also seen in March in air masses with N_2O = 270–320 ppbv sampled at DC-8 altitudes. (Only a few data were obtained in January in air masses with N_2O = 270–320 ppbv at DC-8 altitudes). The downward shift of nitrification altitudes is attributed to the same two factors affecting the denitrification profiles, i.e., the diabatic descent of the Arctic air mass and colder temperatures in February at lower altitudes. Minimum temperatures at 350–380 K (~13–15.5 km) were lower in February than in January, and fell below T_{NAT} continuously only in February and the beginning of March. As a result, PSC particles could efficiently fall to lower altitudes only in February. Considering that the vortex edge was often located near Kiruna, more intensive nitrification than that observed by the ER-2 was possible in the center of the vortex, where atmospheric temperature was lower, as in the case for the winter of 1996/1997 [*Irie et al.*, 2001]. The observations from the DC-8 indicate that nitrification extended to altitudes as low as 10–12.5 km over a wide area in late February/March 2000. This is further confirmed by model calculations, as described below (section 4.3).

4.3. Results From Model Calculations

[23] In Figures 10a and 10b, vertical profiles of redistributed NO_y calculated with the model are shown for 16 January and 27 February, respectively. These two days were selected because 16 January (January deployment) was the day on which air masses with N_2O = 280–290 ppbv were observed with no increase in NO_y from the DC-8, while 27 February (March deployment) was the day on which air masses in the same N_2O range were observed with a clear increase in NO_y (~1 ppbv). NO_y^* was calculated using the MkIV/ER-2 reference relationship. In these figures, results from the two model cases are shown, i.e., the case in which the process leading to denitrification is included (denitrification ON) and the case in which the process is disabled (denitrification OFF). In the 16 January case, denitrification is seen at altitudes above 20 km and nitrification is seen between 14 and 20 km. The increase was limited to altitudes above 14 km because high temperatures prevent PSC particles from descending to lower altitudes. In contrast, nitrification is seen down to 10 km in the 27 February case. This was caused by two factors, as described in section 4.2. First, low temperatures at 12–15 km in February allow PSC particles to fall to lower altitudes more efficiently than they did in January. Second, diabatic descent in the Arctic vortex brought air masses influenced by nitrification to slightly lower altitudes. It is noted that the altitude range of nitrification should generally be well simulated because nitrification occurs when PSC particles encounter temperatures above T_{NAT}, and this process is reliably reproduced by the model. Negative ΔNO_y values in the denitrification-OFF case were due to the mixing of air masses in the region where NO_y and N_2O had a nonlinear relationship [*Michelsen et al.*, 1998; *Kondo et al.*, 1999; *Rex et al.*, 1999].

[24] In Figures 11a and 11b, scatterplots between the model-calculated NO_y and N_2O are shown for the 16 January and 27 February cases. For these plots, model values along the DC-8 flight track were extracted. As already described above (section 4.1), the NO_y-N_2O relationships are quite similar between the January and March cases when denitrification is switched off. When the results from the denitrification-ON and -OFF cases are compared,

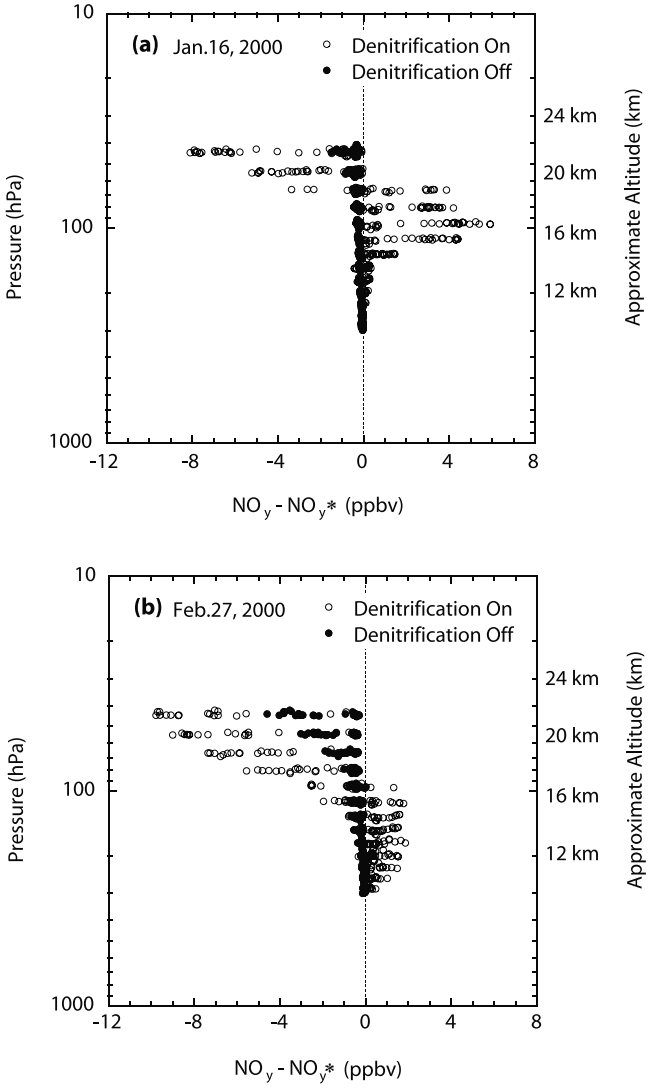

Figure 10. Vertical profiles of redistributed NO_y ($\Delta NO_y = NO_y - NO_y^*$) calculated for the results from CTM (REPROBUS) calculations. The results are shown for the (a) 16 January and (b) 27 February cases.

it is found that denitrification caused only a small change in the NO_y values in the 16 January case at DC-8 altitudes. In contrast, in the 27 February case, an increase in the NO_y values is seen when the denitrification process is included. The ΔNO_y value is 0.5–1.0 ppbv in air masses with N_2O = 280–290 ppbv, which is in good agreement with the measurements (Figure 5 and Figure 6), although the scatter in the NO_y values is greater than the observations (see discussion in section 4.4). The good agreement of the model-calculated NO_y-N_2O correlation with the observations both in the January and March deployments further confirms our interpretation that the increase in NO_y observed from the DC-8 in late February/March was due to NO_y redistribution.

[25] In our model calculations, the number density of NAT particles, which were allowed to form on condensation nuclei, was limited to 5×10^{-3} particles cm^{-3}. This density was chosen because it gave the best agreement with observations in the similar large-scale, three-dimensional model calculations for the Arctic winter stratosphere by *Waibel et al.* [1999]. We performed various sensitivity tests to evaluate the impact of the assumed NAT number density. When a factor of 10 greater NAT particle density is assumed (5×10^{-2} particles cm^{-3}), the degree of nitrification becomes too small (one third of the observed NO_y increase) for the 27 February case; when a factor of 10 smaller density is assumed (5×10^{-4} particles cm^{-3}), the degree of nitrification becomes too large (0.5–0.8-ppbv increase in air masses with N_2O = 280–290 ppbv) for the 16 January case. This was because the greater (smaller) number density of NAT particles resulted in

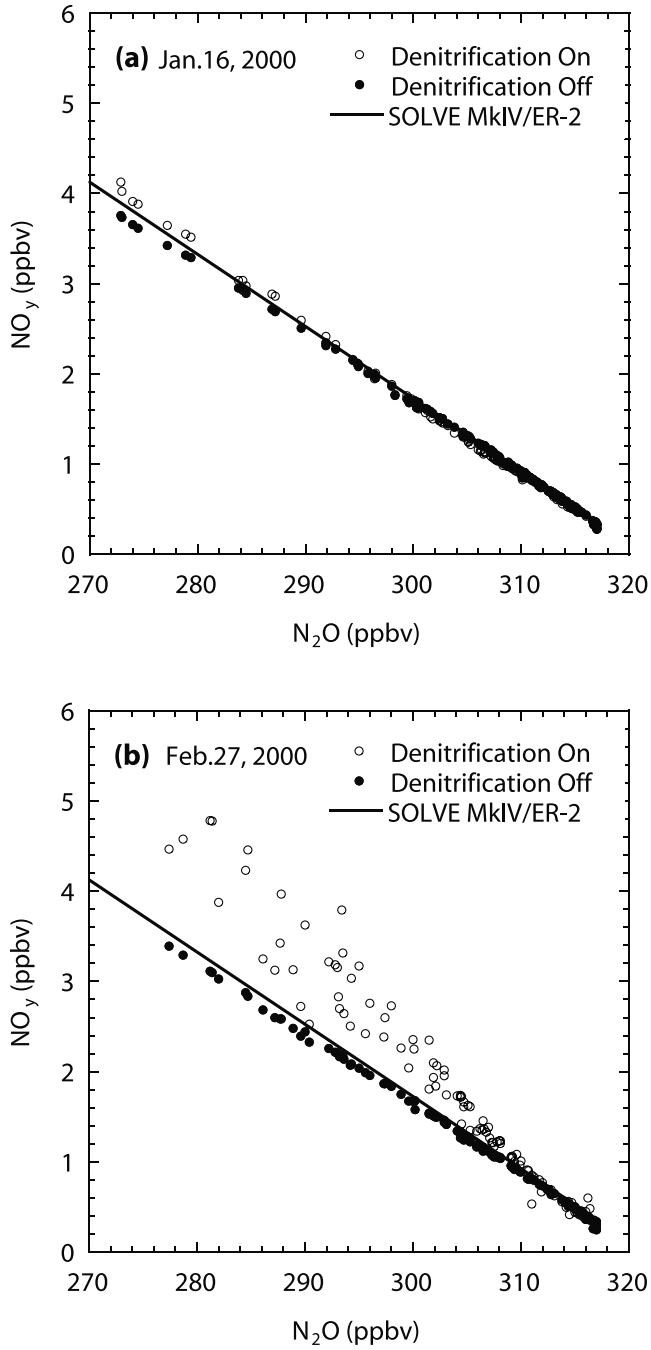

Figure 11. Scatterplot between CTM-calculated NO_y and N_2O values along the DC-8 flight track. The results are shown for the (a) 16 January and (b) 27 February cases.

smaller (larger) particle diameters owing to the limited amount of condensable material, HNO_3 and H_2O. Particles with large diameters (maximum of about 10 μm in our calculation) resulted in effective denitrification and nitrification. It is noted that in both this study and study by *Waibel et al.* [1999], the best agreement between the large-scale model calculations and observations was achieved when a NAT density of 5×10^{-3} particles cm^{-3} was assumed.

[26] *Fahey et al.* [2001] showed that the HNO_3-containing particles in the 1999/2000 Arctic winter stratosphere likely had two particle size modes: the larger mode with a mean diameter of 14.5 μm and a number density of 2.3×10^{-4} particles cm^{-3}, and the smaller mode at 3.5 μm with a number density of 2×10^{-3} particles cm^{-3} (uncertainty of ±30%). The best guess NAT density (5×10^{-3} particles cm^{-3}) in the present study is therefore systematically greater than these observed particle densities. Because of the rather simple treatment of particle growth in the REPROBUS model, the NAT density used in the model may not be directly comparable to the observations. However, the difference between the observations and model calculations provides a range of uncertainties in the NAT particle density causing denitrification and nitrification.

4.4. Processes of NO_y Redistribution

[27] In this section, we explain two observed features: first, a difference in time between the first observation of denitrified air from the ER-2 (20 January) and the first observation of nitrification influence from the DC-8 (27 February), and second, the compactness of the NO_y-N_2O correlation observed from the DC-8 in late February/March, in spite of the sporadic nature of the nitrification processes.

[28] The first ER-2 measurement within the Arctic vortex in the 1999/2000 winter was made on 20 January, in which severely denitrified air masses were observed, indicating that denitrification started prior to this measurement. The nucleation of NAT and NAD at temperatures near T_{ICE} was indicated by laboratory experiments [*Worsnop et al.*, 1993; *Salcedo et al.*, 2001]. Selective nucleation of these particles and subsequent particle growth can cause denitrification [*Waibel et al.*, 1999; *Tabazadeh et al.*, 2001]. In fact, recent satellite measurements have shown that denitrification occurred only in air masses that experienced temperatures near T_{ICE} [*Kondo et al.*, 2000; *Irie et al.*, 2001]. The minimum temperature in the Arctic at 475 K potential temperature was near or below T_{ICE} from the end of December (Figures 3 and 4). Consequently, denitrification must have started at that time.

[29] The January DC-8 measurements made between 14 and 29 January (Table 1) showed no clear increase in NO_y in this period (Figures 5 and 6). The clear increase in NO_y was observed for the first time during the 27 February flight (transit into Kiruna), which was the first flight during the March deployment. No DC-8 data are available between 29 January and 27 February.

[30] The absence of significant nitrification at DC-8 altitudes in January was primarily because temperatures between 350 and 380 K (~13.5–15.5 km) were generally high in January (Figures 3 and 4), and almost all of the PSC particles had evaporated at altitudes above 12.5 km, as described in sections 4.2 and 4.3. In February, the Arctic minimum temperatures were continuously lower than T_{NAT} at altitudes as low as 350 K (~13.5 km), enabling more particles to fall efficiently to DC-8 altitudes. Consequently, the redistribution process, which occurred in February, should be partly responsible for the observed increase in the NO_y level in late February/March.

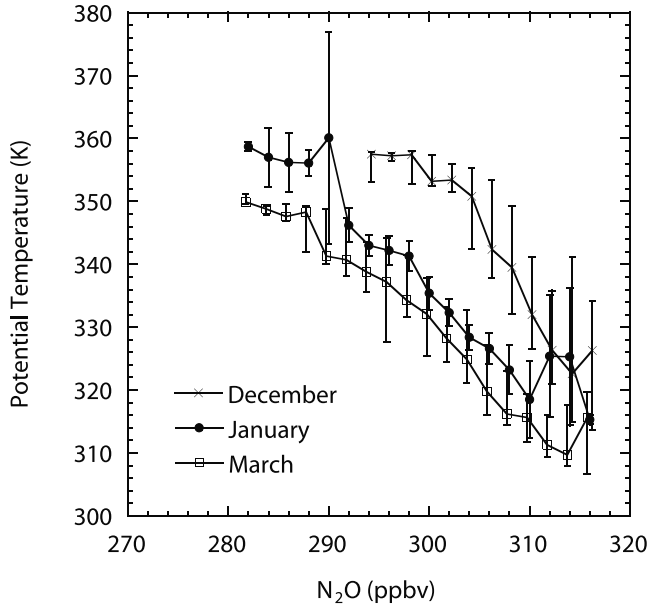

Figure 12. The N_2O mixing ratio observed from the DC-8 versus potential temperature. Median values of potential temperature for various N_2O ranges are shown. The vertical bars are the 67% ranges of the potential temperature.

[31] Diabatic descent of nitrified air masses can also partly account for the delay of the first observation of the NO_y redistribution at DC-8 altitudes. Because temperatures at 475 K (~21 km), where intensive denitrification was observed (Figure 9b), were close to or below T_{ICE} only until the end of January and were well above T_{ICE} in February, denitrification must have been less intense in February. In fact, although large HNO_3-containing particles with diameters of 10 to 20 μm were detected from the ER-2 between 20 January and 7 March in a total of seven flights, the number and spatial extent of these particles were significantly less after 20 January [*Fahey et al.*, 2001]. Consequently, if nitrification occurred just above the DC-8 altitude in January, a slight diabatic descent could lead to the NO_y increase in late February/March.

[32] The N_2O mixing ratios observed from the DC-8 are shown versus potential temperature in Figure 12. In this figure, median values of potential temperature for various N_2O ranges are shown for the three DC-8 deployments. The change in the potential temperature in air masses with N_2O = 280–290 ppbv was about 8 K between the January and March deployments (44 days apart). Assuming this change was solely due to diabatic cooling, it corresponded to an altitude displacement of 0.5–0.8 km. A similar change in the potential temperature was also detected from the unified N_2O measurements from the ER-2 in air masses with N_2O = 250 ppbv for the same time period [*Greenblatt et al.*, 2002]. A similar change was also detected between mid-January and mid-February 1992 from the DC-8 N_2O measurements made during AASE 2 [*Collins et al.*, 1993]. Figure 12 also

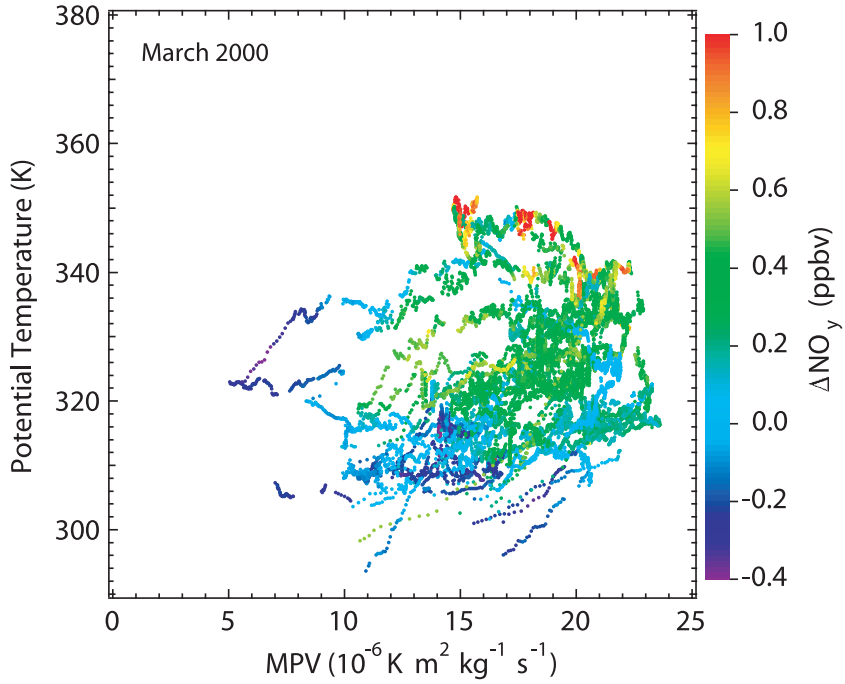

Figure 13. Redistributed NO_y (ΔNO_y) as a function of potential temperature and modified potential vorticity (MPV) derived from the DC-8 measurements during the March deployment. Note that data shown using the highest color code (red) include ΔNO_y values greater than 1 ppbv.

shows that the altitude displacement was greater between the December and January deployments (1.0–1.7 km for air masses with N_2O = 294–300 ppbv). As described above, denitrification quite likely started at the end of December. Air masses that were influenced by nitrification earlier in the winter could descend farther by the time of the late February/March observations. On the other hand, the altitude regions where PSC particles evaporated were generally high in early winter, as seen in Figures 3 and 4, indicating that nitrified air masses needed to descend relatively long vertical distances to be observed from the DC-8. Influence of the diabatic descent of nitrified air masses was therefore critically determined by the vertical structure of the temperature field and its temporal change through the winter.

[33] The compactness of the NO_y-N_2O relationship observed from the DC-8 in late February/March is now examined. From the discussion above, PSC particles likely fell to above DC-8 altitudes in December and January and as low as DC-8 altitudes in February. When PSC particles evaporated within a particular altitude layer, the effects were initially confined to a limited horizontal area, and the NO_y-N_2O correlation became inhomogeneous in that layer. Consequently, the observed compactness indicates that air masses influenced by nitrification were generally well mixed with surrounding air masses so that local enhancements in the NO_y-N_2O correlation diminished before the DC-8 observations in late February/March.

[34] In Figure 13, the ΔNO_y values obtained in the March deployment are shown as a function of potential temperature and modified potential vorticity (MPV, defined by *Lait* [1994] and θ_0 = 420 K was assumed). As anticipated from the correlations of ΔNO_y and N_2O (Figure 6) and of N_2O and potential temperature (Figure 12), higher ΔNO_y values were generally found at higher potential temperatures. Figure 13 also shows that the ΔNO_y values on each of the isentropic surfaces were relatively uniform, especially in air masses with MPV = 12–23 PV units (10^{-6} K m^2 $kg^{-1}s^{-1}$) at potential temperatures of 320–350 K. The average ΔNO_y value in these air masses was 400 ± 196 pptv. This result further confirms that air-mixing processes tended to homogenize the influence from nitrification in space by the time of March deployment.

[35] Model calculations provide some insights into the redistribution and mixing processes. In Figure 14, the results from the two model cases are shown for the 27 February flight track, i.e., the case in which the process leading to denitrification is activated only between December 1999 and January 2000 and the case in which the process is activated only in February 2000. As seen in this figure, the denitrification process, both in December–January and February, likely contributed to the observed increase in NO_y. The process in December–January resulted in a systematic increase in NO_y in air masses with N_2O < 305 ppbv, and the resulting NO_y-N_2O relationship is compact, presumably due to mixing processes. On the other hand, the process in February resulted in a sporadic increase in NO_y in air masses with N_2O < 295 ppbv and the resulting NO_y-N_2O relationship has a relatively large standard deviation, presumably due to a mixing time insufficient to achieve a compact relationship. Considering the compactness of the N_2O-NO_y relationship observed in late February/March, the process in December–January could have contributed more to the observed increase in NO_y.

4.5. Comparison with Earlier Measurements

[36] In Figures 15a and 15b, the N_2O-NO_y relationships obtained in earlier measurements in the Arctic or northern midlatitudes are shown with the median SOLVE/DC-8

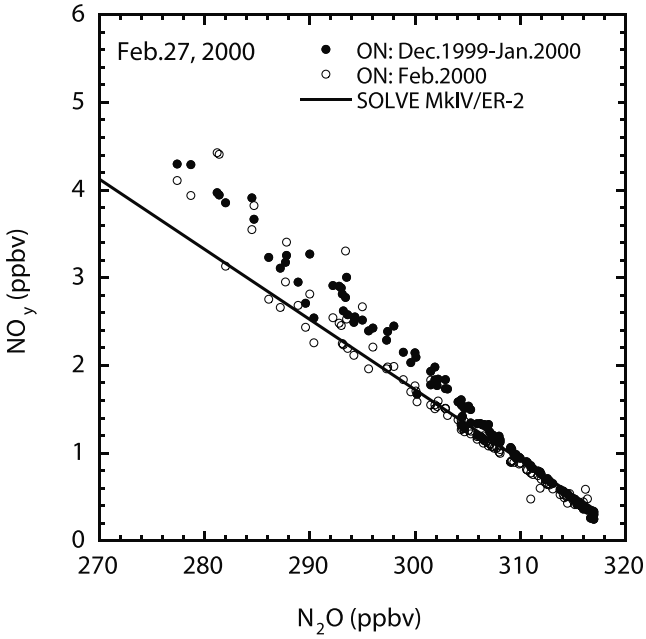

Figure 14. Scatterplot between CTM-calculated NO_y and N_2O along the DC-8 flight track for the 27 February case. The results from two model calculations are shown: The case in which the process leading to denitrification is activated only between December 1999 and January 2000 (closed circles), and the case in which the process is activated only in February 2000 (open circles).

NO_y-N_2O values. For these plots, N_2O values in earlier measurements were scaled due to an interannually increasing trend of N_2O in the troposphere by 0.5 ppbv/year [*Ishijima et al.*, 2001].

[37] Figure 15a shows that the high NO_y values, as well as the steep dNO_y/dN_2O gradient, observed in March 2000 have not been observed before in the Arctic and northern midlatitudes from either the DC-8 or the ER-2. During AASE 1, conducted over the Arctic in January and early February 1989, episodic events of unusually high NO_y values with mixing ratios between 3 and 12 ppbv were observed from the DC-8 at altitudes of 10–12.5 km during several flights late in that mission [*Hübler et al.*, 1990]. In one of the significant cases, NO_y levels were elevated for about 30 min (390 km along the flight track). Substantial denitrification inside the Arctic vortex was observed by the ER-2 during that winter, and the observed NO_y increase was attributed to a redistribution of NO_y. Although O_3 and N_2O data were limited, the observed local enhancements in the NO_y/O_3 and NO_y/NO_y* ratios indicate that these air masses had recently been influenced by the evaporation of PSC particles and had not yet been diluted with surrounding air. From its nature, individual nitrification events occur within a limited time and space. The accumulation of these events and mixing processes will result in the systematic increase in NO_y and compact correlation between NO_y and N_2O, as observed during SOLVE.

[38] AASE 2 was conducted over the Arctic between January and March 1992. Very similar N_2O-NO_y relationships were observed from the DC-8 in January and March, although systematically lower NO_y values were observed in February [*Weinheimer et al.*, 1993]. They showed that the very small change in the NO_y-N_2O relationship was consistent with the fact that denitrification was less extensive in that year. In fact, the AASE 2 N_2O-NO_y relationship is similar to the SOLVE MkIV/ER-2 relationship (Figure 15a).

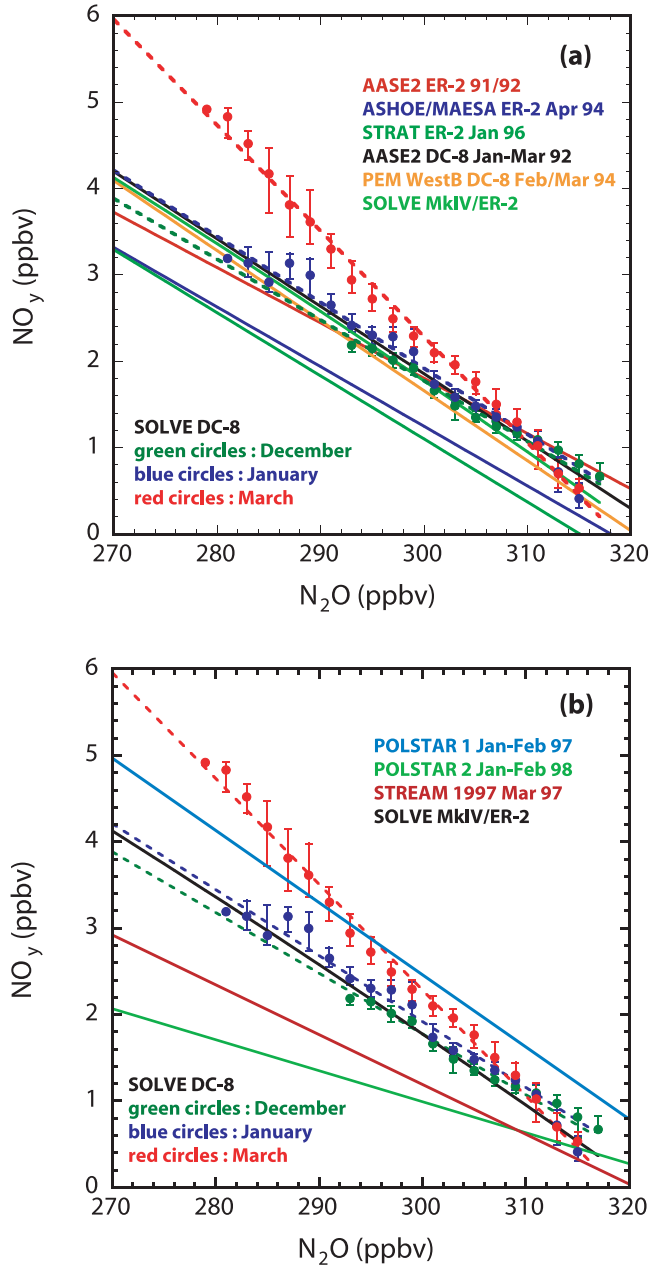

Figure 15. Median values of NO_y for various N_2O ranges obtained from the SOLVE/DC-8 measurements, which are compared with results obtained from earlier aircraft measurements. N_2O values in earlier measurements were scaled due to an interannually increasing trend of N_2O of 0.5 ppbv/year [*Ishijima et al.*, 2001]. (a) Relationships obtained in earlier DC-8 and ER-2 measurements are shown, adapted from *Keim et al.* [1997], *Weinheimer et al.* [1993], and *Singh et al.* [1997]. (b) Relationships obtained in earlier European campaigns are shown, adapted from *Zieries et al.* [2000] and *Fischer et al.* [2000].

[39] During the Polar Stratosphere Aerosol Experiment 1 (pOLSTAR 1) campaign (January and February 1997), NO_y values systematically higher than the earlier measurements were observed in the Arctic at potential temperatures between about 340 and 360 K from the Deutsches Zentrum fur Luft- und Raumfahrt (DLR) Falcon aircraft [*Ziereis et al.*, 2000]. The NO_y values were systematically higher than the SOLVE Mk-IV/ER-2 values by about 1 ppbv (Figure 15b). In this case, the dNO_y/dN_2O gradient was similar to those from the earlier DC-8 and ER-2 measurements, and the increase in NO_y appeared with a positive offset. Because temperatures at 50 hPa during the 1996/1997 Arctic winter did not fall below T_{NAT} before mid-January, which was just before the Falcon measurements, aircraft emissions were proposed as a source of reactive nitrogen [*Ziereis et al.*, 2000].

[40] Nitrification was clearly detected from satellite measurements in the 1996/1997 Arctic winter at 12–16 km between mid-February and the beginning of March, soon after denitrification was observed at altitudes between 17 and 22 km [*Kondo et al.*, 2000; *Irie et al.*, 2001]. The area where the temperature was lower than T_{NAT} extended to as low as 13 km in February and increases in HNO_3 of about 1 ppbv were observed at the 370-K isentropic surface ($\sim$13 km) at equivalent latitudes higher than 65°N. As in the 1999/2000 winter, the vertical temperature profile largely controlled the vertical extent of the nitrification influences.

5. Summary and Conclusions

[41] During the SOLVE campaign, measurements of NO_y, N_2O, and O_3 were made in the Arctic lower stratosphere at altitudes between 6 and 12.5 km from the NASA DC-8 aircraft in December 1999 and January and late February/March 2000. In January and late February/March, measurements were also made at altitudes up to 21 km from the ER-2 aircraft.

[42] The N_2O mixing ratio measured from the DC-8 ranged between 280 and 320 ppbv. The NO_y-N_2O correlations obtained in the December and January deployments were comparable and were also similar to the reference correlation established using the MkIV balloon measurements made during SOLVE prior to the onset of denitrification, which was in good agreement with the ER-2 extra-vortex measurements. During the March deployment, NO_y values obtained from the DC-8 were slightly higher systematically than those observed during the previous deployments, although a compact correlation between NO_y and N_2O was maintained. The increase in NO_y ($\Delta NO_y = NO_y - NO_y^*$ was especially evident (0.5 to 1 ppbv) in air masses with N_2O values of 280–290 ppbv (altitudes of 11.0–12.5 km and potential temperature of 340–350 K).

[43] The daily minimum temperatures at 450–500 K ($\sim$20–22 km) in the Arctic fell below T_{ICE} between late December and mid-January, and intensive denitrification was observed from the ER-2 at altitudes between 17 and 21 km in January and March [*Popp et al.*, 2001]. In fact, large HNO_3-containing particles with diameters of 10 to 20 μm were detected from the ER-2 between 20 January and 7 March [*Fahey et al.*, 2001]. The number and spatial extent of these particles were significantly less after 20 January, in accordance with the increase in temperatures. Although measurements at altitudes below 16 km were limited to over northern Scandinavia, they show increases in NO_y due to nitrification at 15–18 km and 14–16.5 km in January and March, respectively [*Popp et al.*, 2001]. Considering that the vortex edge was often located near Kiruna, more intensive nitrification than that observed by the ER-2 was possible in the center of the vortex, where atmospheric temperatures were lower. The observed results presented in this paper indicate that nitrification extended to altitudes as low as 10–12.5 km over the wide area in the 1999/2000 Arctic winter.

[44] The significant effect of nitrification was observed only in late February/March at DC-8 altitudes, primarily because temperatures between 350 and 380 K ($\sim$13.5–15.5 km) were generally high in January, and almost all of the PSC particles had evaporated at altitudes above 12.5 km. Because of the severe denitrification in January, nitrification, which occurred just above the DC-8 altitudes, followed by the diabatic descent of air, was considered to partly account for the observed increase in NO_y in late February/March. In February, the Arctic minimum temperatures were continuously lower than T_{NAT} at altitudes as low as 350 K ($\sim$13.5 km), and more particles could efficiently fall to DC-8 altitudes, although ongoing denitrification was likely to be less intense, according to the ER-2 PSC particle measurements. Air masses influenced by nitrification were well mixed with surrounding air masses and the compact correlation between NO_y and N_2O was established before the DC-8 March deployment. The average increase in NO_y (ΔNO_y) was 400 pptv in air masses with MPV of 12–23 PV units (10^{-6} K m^2 kg^{-1}s^{-1}) at potential temperatures of 320–350 K.

[45] The observed features are generally reproduced well by the REPROBUS 3-D CTM only when the denitrification process was included. In particular, the good agreement of the model-calculated NO_y-N_2O correlations with the observations in both the January and March deployments confirmed our interpretation that the increase in NO_y observed from the DC-8 in late February/March was due to the redistribution of NO_y.

[46] The results presented in this paper show the redistribution processes in the 1999/2000 Arctic winter affected the NO_y levels at altitudes as low as 10–12 km over a wide area. The wide spread influence at these low altitudes was never observed during previous NASA/DC-8 and ER-2 observations in accordance with unusually cold temperatures in the 1999/2000 Arctic stratosphere. The results presented in this paper also show that the vertical structure of the temperature field is a critical factor determining the vertical extent of the NO_y redistribution.

[47] **Acknowledgments.** We are indebted to all SOLVE participants for their cooperation and support. Special thanks are due to the flight and ground crews of the NASA DC-8 for helping make this effort a success. We thank T. Wada for his assistance with the data analyses and N. Toriyama, M. Kanada, and H. Jindo for their technical assistance with NO_y measurements. We also thank D. W. Fahey and R. S. Gao at the NOAA Aeronomy Laboratory for providing ER-2 NO_y data, D. Hurst and J. Elkins at NOAA CMDL, S. Schauffler and E. Atlas at NCAR, H. Jost at NASA ARC, C. Webster and R. Herman at JPL, and J. Greenblatt at Princeton University for providing ER-2 unified N_2O data. We also thank P. A. Newman at NASA GSFC for calculating the modified potential vorticity values along the DC-8 flight track. We also thank R. Selkirk at NASA ARC for providing GEOS-3 meteorological analysis prepared for the SOLVE mission by the Data Assimilation Office (DAO) at NASA GSFC. The meteorological data were supplied by the European Center for Medium-Range Weather Forecasts (ECMWF) and the Norwegian Institute for Air Research (NILU). The modeling work presented in this study was supported by the European Union through the THESEO-2000/Eurosolve

project. This work was also supported in part by the Ministry of Education, Science, Sports, and Culture (MESSC).

References

Abrams, M. C., et al., Trace gas transport in the Arctic vortex inferred from ATMOS ATLAS-2 observations during April 1993, *Geophys. Res. Lett.*, *23*, 2345–2348, 1996.

Carslaw, K. S., B. P. Luo, S. L. Clegg, T. Peter, P. Brimblecombe, and P. J. Crutzen, Stratospheric aerosol growth and HNO_3 gas phase depletion from coupled HNO_3 and water uptake by liquid particles, *Geophys. Res. Lett.*, *21*, 2479–2482, 1994.

Carslaw, K. S., S. B. Luo, and T. Peter, An analytic expression for the composition of aqueous HNO_3-H_2SO_4 stratospheric aerosols including gas phase removal of HNO_3, *Geophys. Res. Lett.*, *22*, 1877–1880, 1995.

Carslaw, K. S., T. Peter, and S. L. Clegg, Modeling the composition of liquid stratospheric aerosols, *Rev. Geophys.*, *35*, 125–154, 1997.

Collins, J. E., G. W. Sachse, B. E. Anderson, A. J. Weinheimer, J. G. Walega, and B. A. Ridley, AASE-II in situ tracer correlation of methane, nitrous oxide, and ozone as observed aboard the DC-8, *Geophys. Res. Lett.*, *20*, 2543–2546, 1993.

Del Negro, L. A., et al., Evaluating the role of NAT, NAD, and liquid H_2SO_4/H_2O/HNO_3 solutions in Antarctic polar stratospheric cloud aerosol: Observations and implications, *J. Geophys. Res.*, *102*, 13,255–13,282, 1997.

DeMore, W. B., S. P. Spander, D. M. Golden, R. F. Hampson, M. J. Kurylo, C. J. Howard, A. R. Ravishankara, C. E. Kolb, and M. J. Molina, Chemical kinetics and photochemical data for use in stratospheric modeling, *JPL Publ.*, *97-4*, 266 pp., 1997.

Drdla, K., A. Tabazadeh, R. P. Turco, M. Z. Jacobson, J. E. Dye, C. Twohy, and D. Baumgardner, Analysis of the physical state of one Arctic polar stratospheric cloud based on observations, *Geophys. Res. Lett.*, *21*, 2475–2478, 1994.

Fahey, D. W., et al., In situ measurements of total reactive nitrogen, total water, and aerosol in a polar stratospheric cloud in the Antarctic, *J. Geophys. Res.*, *94*, 11,299–11,315, 1989.

Fahey, D. W., et al., Observations of denitrification and dehydration in the winter polar stratospheres, *Nature*, *344*, 321–324, 1990.

Fahey, D. W., et al., The detection of large HNO_3-containing particles in the winter Arctic stratosphere, *Science*, *291*, 1026–1031, 2001.

Fischer, H., F. G. Wienhold, P. Hoor, O. Bujok, C. Schiller, P. Siegmund, M. Ambaum, H. A. Sheeren, and J. Lelieveld, Tracer correlations in the northern high latitude lowermost stratosphere: Influence of cross-tropopause mass exchange, *Geophys. Res. Lett.*, *27*, 97–100, 2000.

Gao, R. S., et al., Observational evidence for the role of denitrification in Arctic stratospheric ozone loss, *Geophys. Res. Lett.*, *28*, 2879–2882, 2001.

Greenblatt, J. B., et al., Tracer-based determination of vortex descent in the 1999/2000 Arctic winter, *107*, 10.1029/2001JD000937, in press, 2002.

Hanson, D., and K. Mauersberger, Laboratory studies of the nitric acid trihydrate: Implications for the south polar stratosphere, *Geophys. Res. Lett.*, *15*, 855–858, 1988.

Hintsa, E. J., et al., Dehydration and denitrification in the Arctic polar vortex during the 1995/1996 winter, *Geophys. Res. Lett.*, *25*, 501–504, 1998.

Hübler, G., et al., Redistribution of reactive odd nitrogen in the lower Arctic stratosphere, *Geophys. Res. Lett.*, *17*, 453–456, 1990.

Hurst, D. F., et al., Constructing a unified, high-resolution nitrous oxide data set for ER-2 flights during SOLVE, *107*, 10.1029/2001JD000417, in press, 2002.

Irie, H., M. Koike, Y. Kondo, G. E. Bodeker, M. Y. Danilin, and Y. Sasano, Redistribution of nitric acid in the Arctic lower stratosphere during the winter of 1996/1997, *J. Geophys. Res.*, *106*, 23,139–23,150, 2001.

Ishijima, K., T. Nakazawa, S. Sugawara, S. Aoki, and T. Saeki, Concentration variations of tropospheric nitrous oxide over Japan, *Geophys. Res. Lett.*, *28*, 171–174, 2001.

Kawa, S. R., D. W. Fahey, K. K. Kelly, J. E. Dye, D. Baumgardner, B. W. Gandrud, M. Loewenstein, G. V. Ferry, and K. R. Chan, The Arctic polar stratospheric cloud aerosol: Aircraft measurements of reactive nitrogen, total water, and particles, *J. Geophys. Res.*, *97*, 7925–7938, 1992.

Keim, E. R., et al., Measurements of the NO_y-N_2O correlation in the lower stratosphere: Latitudinal and seasonal changes and model comparisons, *J. Geophys. Res.*, *102*, 13,193–13,212, 1997.

Koike, M., et al., Impact of aircraft emissions on reactive nitrogen over the North Atlantic Flight Corridor region, *J. Geophys. Res.*, *105*, 3665–3677, 2000.

Kondo, Y., S. Kawakami, M. Koike, D. W. Fahey, H. Nakajima, N. Toriyama, M. Kanada, Y. Zhao, G. W. Sachse, and G. L. Gregory, The performance of an aircraft instrument for the measurement of NO_y, *J. Geophys. Res.*, *102*, 28,663–28,671, 1997.

Kondo, Y., et al., NO_y-N_2O correlation observed inside the Arctic vortex in February 1997: Dynamical and chemical effects, *J. Geophys. Res.*, *104*, 8215–8224, 1999.

Kondo, Y., H. Irie, M. Koike, and G. E. Bodeker, Denitrification and nitrification in the Arctic stratosphere during the winter of 1996/1997, *Geophys. Res. Lett.*, *27*, 337–340, 2000.

Lait, L. R., An alternative form for potential vorticity, *J. Atmos. Sci.*, *51*, 1754–1759, 1994.

Lefevre, F., G. Brasseur, I. Folkins, A. K. Smithand, and P. Simon, Chemistry of the 1991/1992 stratospheric winter: Three-dimensional model simulations, *J. Geophys. Res.*, *99*, 8183–8195, 1994.

Lefevre, F., F. Figarol, K. S. Carslaw, and T. Peter, The 1997 Arctic ozone depletion quantified from three-dimensional model simulations, *Geophys. Res. Lett.*, *25*, 2425–2428, 1998.

Manny, G. L., and L. Sabutis, Development of the polar vortex in the 1999/2000 Arctic winter stratosphere, *Geophys. Res. Lett.*, *27*, 2589–2592, 2000.

Marti, J., and K. Mauersberger, A survey and new measurements of ice vapor pressure at temperatures between 170 and 250 K, *Geophys. Res. Lett.*, *20*, 363–366, 1993.

Michelsen, H. A., G. L. Manney, R. M. Gunseon, and R. Zander, Correlations of stratospheric abundances of NO_y, O_3, N_2O, and CH_4, derived from ATMOS measurements, *J. Geophys. Res.*, *103*, 28,347–28,359, 1998.

Nash, E. R., P. A. Newman, J. E. Rosenfield, and M. R. Schoeberl, An objective determination of the polar vortex using Ertel's potential vorticity, *J. Geophys. Res.*, *101*, 9471–9478, 1996.

Newman, P. A., et al., An overview of the SOLVE-THESEO 2000 campaign, *J. Geophys.*, *107*, 10.1029/2001JD001303, in press, 2002.

Popp, P. J., et al., Severe and extensive denitrification in the 1999/2000 Arctic winter stratosphere, *Geophys. Res. Lett.*, *28*, 2875–2878, 2001.

Rex, M., et al., Prolonged stratospheric ozone loss in the 1995–96 Arctic winter, *Nature*, *389*, 835–838, 1997.

Rex, M., et al., Subsidence, mixing, and denitrification of Arctic polar vortex air measured during POLARIS, *J. Geophys. Res.*, *104*, 26,611–26,623, 1999.

Richard, E. C., et al., Severe chemical ozone loss inside the Arctic polar vortex during winter 1999/2000 inferred from in situ airborne measurements, *Geophys. Res. Lett.*, *28*, 2197–2200, 2001.

Rosenfield, J. E., P. A. Newman, and M. R. Schoeberl, Computations of diabatic descent in the stratospheric polar vortex, *J. Geophys. Res.*, *99*, 16,677–16,689, 1994.

Salawitch, R. J., et al., Chemical loss of ozone in the Arctic polar vortex in the winter of 1991–1992, *Science*, *261*, 1146–1149, 1993.

Salawitch, R. J., et al., Chemical loss of ozone during the Arctic winter of 1999/2000: An analysis based on balloon-borne observations, *J. Geophys. Res.*, *107*, *107*, 10.1029/2001JD000620, in press, 2002.

Salcedo, D., L. T. Molina, and M. J. Molina, Homogeneous freezing of concentrated aqueous nitric acid solutions at polar stratospheric temperatures, *J. Phys. Chem.*, *105*, 1433–1439, 2001.

Sander, S. P., et al., Chemical kinetics and photochemical data for use in stratospheric modeling, *JPL Publ.*, *00-3*, 74 pp., 2000.

Santee, M. L., G. L. Manney, N. J. Livesey, and J. W. Waters, UARS microwave limb sounder observations of denitrification and ozone loss in the 2000 Arctic late winter, *Geophys. Res. Lett.*, *27*, 3213–3216, 2000.

Schoeberl, M. R., L. R. Lait, P. A. Newman, and J. E. Rosenfield, Structure of the polar vortex, *J. Geophys. Res.*, *97*, 7859–7882, 1992.

Singh, H. B., et al., Trace chemical measurements from the northern midlatitude lowermost stratosphere in the early spring: Distribution, correlation, and fate, *Geophys. Res. Lett.*, *24*, 103–127, 1997.

Sinnhuber, B. M., et al., Large loss of total ozone during the Arctic winter of 1999/2000, *Geophys. Res. Lett.*, *27*, 3473–3476, 2000.

Sugita, T., Y. Kondo, H. Nakajima, U. Schmidt, A. Engel, H. Oelhaf, G. Wetzel, M. Koike, and P. A. Newman, Denitrification observed inside the Arctic vortex in February 1995, *J. Geophys. Res.*, *103*, 16,221–16,233, 1998.

Tabazadeh, A., R. P. Turco, K. Drdla, M. Z. Jacobson, and O. B. Toon, A study of type I polar stratospheric cloud formation, *Geophys. Res. Lett.*, *21*, 1619–1622, 1994.

Tabazadeh, A., M. L. Santee, M. Y. Danilin, H. C. Pumphrey, P. A. Newman, P. J. Hamill, and J. L. Mergenthaler, Quantifying denitrification and its effect on ozone recovery, *Science*, *288*, 1407–1411, 2000.

Tabazadeh, A., E. J. Jensen, O. B. Toon, K. Drdla, and M. R. Schoeberl, Role of the stratospheric polar freezing belt in denitrification, *Science*, *291*, 2591–2594, 2001.

Vay, S. A., B. E. Anderson, G. W. Sachse, J. E. Collins Jr., J. R. Podolske, C. H. Twohy, B. Gandrud, K. R. Chan, S. L. Baughcum, and H. A. Wallio, DC-8-based observations of aircraft CO, CH_4, N_2O, and H_2O(g) emission indices during SUCCESS, *Geophys. Res. Lett.*, *25*, 1717–1720, 1998.

Waibel, A. E., T. Peter, K. S. Carslaw, H. Oelhaf, G. Wetzel, P. J. Crutzen, U. Pöschl, A. Tsias, E. Reimer, and H. Fischer, Arctic ozone loss due to denitrification, *Science*, *283*, 2064–2069, 1999.

Weinheimer, A. J., J. G. Walega, B. A. Ridley, G. W. Sachse, B. E. Anderson, and J. E. Collins Jr., Stratospheric NO_y measurements on the NASA DC-8 during AASE II, *Geophys. Res. Lett.*, *20*, 2563–2566, 1993.

World Meteorological Organization, *Scientific Assessment of Ozone Depletion,1998*, Natl. Oceanic and Atmos. Admin., Washington, D. C., 1999.

Worsnop, D. R., L. E. Fox, M. S. Zahniser, and S. C. Wofsy, Vapor pressures of solid hydrates of nitric acid: Implications for polar stratospheric clouds, *Science*, *259*, 71–74, 1993.

Ziereis, H., H. Shclager, H. Fischer, C. Feigl, P. Hoor, R. Marquardt, and V. Wagner, Aircraft measurements of tracer correlations in the Arctic subvortex region during the Polar Stratospheric Aerosol Experiment (POLSTAR), *J. Geophys. Res.*, *105*, 24,305–24,313, 2000.

B. E. Anderson, M. A. Avery, and G. W. Sachse, NASA Langley Research Center, Hampton, VA 23681-0001, USA. (b.e.anderson@larc.nasa.gov; m.a.avery@larc.nasa.gov; g.w.sachse@larc.nasa.gov)

J. O. Ballenthin, D. E. Hunton, T. M. Miller, and A. Viggiano, 5 Air Force Research Laboratory/Space Vehicles Directorate, Hanscom Air Force Base, MA 01731, USA. (john.ballenthin@hanscom.af.mil; donald.hunton@hanscom.af.mil; thomas.miller@hanscom.af.mil; albert.viggiano@hanscom.af.mil)

H. Ikeda, Y. Kondo, and N. Takegawa, Research Center for Advanced Science and Technology, University of Tokyo, 4-6-1 Komaba, Meguro, Tokyo 153-8904, Japan. (hibiki@atmos.rcast.u-tokyo.ac.jp; kondo@atmos.rcast.u-tokyo.ac.jp; takegawa@stelab.nagoya-u.ac.jp)

H. Irie, National Institute for Environmental Studies, Satellite Remote Sensing Research Team, 16-2, Onogawa, Tsukuba, Ibaraki 305-8506, Japan. (irie.hitoshi@nies.go.jp)

M. Koike and Y. Masui, Department of Earth and Planetary Science, Graduate School of Science, University of Tokyo, Hongo 7-3-1, Bunkyo-ku, Tokyo 113-0033, Japan. (koike@eps.s.u-tokyo.ac.jp; masui@aos.eps.s.u-tokyo.ac.jp)

F. Lefevre, Service d'Aeronomie, Institut Pierre-Simon Laplace, BP 102, 4 Place Jussieu, 75252 Paris Cedex 05, France. (franck.lefevre@aero.jussieu.fr)